THESIS

ON THE RELATION BETWEEN SATELLITE OBSERVED LIQUID WATER PATH, CLOUD DROPLET NUMBER CONCENTRATION AND CLOUD BASE RAIN RATE AND ITS IMPLICATION FOR THE AUTO-CONVERSION RATE IN STRATOCUMULUS CLOUDS

Submitted by

Yasutaka Murakami

Department of Atmospheric Science

In partial fulfillment of the requirements

For the Degree of Master of Science

Colorado State University

Fort Collins, Colorado

Spring 2020

Master's Committee:

Advisor: Christian D. Kummerow
Co-Advisor: Susan C. van den Heever

Chandrasekaran Venkatachalam

ABSTRACT

ON THE RELATION BETWEEN SATELLITE OBSERVED LIQUID WATER PATH, CLOUD DROPLET NUMBER CONCENTRATION AND CLOUD BASE RAIN RATE AND ITS IMPLICATION FOR THE AUTO-CONVERSION RATE IN STRATOCUMULUS CLOUDS

Stratocumulus clouds are low-level convective clouds that develop within the atmospheric boundary layer. Their persistence and broad coverage of the earth's surface produces important impacts on the global radiation energy budget and hydrological cycle. Precipitation processes of these stratocumulus clouds play a large role in their longevity and spatial distribution through their interaction with the vertical profiles of humidity and temperature within the atmospheric boundary layer. This has led to a number of field campaigns to understand the precipitation processes of stratocumulus clouds. However, because of the limited field campaign domains and limited amount of these observations, it is difficult to draw statistically significant conclusions on the precipitation processes of global stratocumulus clouds from these data. In this study, space-borne observations from A-Train satellites are utilized to obtain robust relations among the liquid water path, cloud droplet number concentration and cloud base rain rate for three geographical regions with similar large-scale environments, namely the north east Pacific off the coast of California, the south east Pacific off the coast of Peru and the south east Atlantic off the coast of Namibia, where strong subsidence flow from the subtropical-high is observed.

Radar reflectivity from CloudSat's Cloud Profiling Radar (CPR) is employed to estimate the cloud base rain rate (R_{cb}). Liquid water path (*LWP*) and cloud droplet number concentration (*Nd*) are estimated from Moderate Resolution Imaging Spectroradiometer (MODIS) cloud optical thickness and effective radius. The relation between cloud base rain rate (R_{cb}) and the ratio of liquid water path to cloud droplet number concentrations (*LWP/Nd*) are obtained from a large

number of A-train observations that show similar probability density distribution for all three target areas in this study. R_{cb} has a positive correlation with *LWP/Nd* and the increase in R_{cb} becomes larger as *LWP/Nd* increases, which is consistent with the results from previous ground-based observations. The research presented here also shows that the increase of R_{cb} in respect to *LWP/Nd* become more gradual in larger *Nd* regions, which suggests that the relation between R_{cb} and *LWP/Nd* changes with different cloud droplet number concentrations. These findings are consistent with our theoretical understanding of cloud physics processes in that 1) auto-conversion and accretion growth of rain embryos becomes more effective as cloud droplet number concentrations near cloud top decrease, and 2) auto-conversion is suppressed when the cloud droplet radius is small enough.

The sensitivity of the auto-conversion rate to cloud droplet number concentration is investigated by examining pixels with small *LWP* in which the accretion process is assumed to have little influence on R_{cb}. The upper limit of the dependency of auto-conversion on the cloud droplet number concentration is assessed from the relation between cloud base rain rate and cloud top droplet number concentration since the sensitivity is exaggerated by the accretion process. The upper limit of the sensitivity of auto-conversion found in this study was found to be a cloud droplet number concentration to the power of -1.44 ± 0.12. This study demonstrates that satellite observations are capable of detecting the average manner in which precipitation processes are modulated by the liquid water path and drop number concentrations.

ACKNOWLEDGEMENTS

I would like to thank Prof. Christian Kummerow and Prof. Susan van den Heever for their mentorship and guidance throughout the completion of this thesis. It was impossible to finish my thesis in this short timeframe without their appropriate guidance. I also thank Prof. Chandrasekaran Venkatachalam for his role on my Master's committee.

I am also grateful to the staff member of the CloudSat Data Processing Center, which is run by Cooperative Institute for Research in the Atmosphere, for their technical assistance to utilize the data. This research was supported by the Japanese Government Long-term Overseas Fellowship Program.

TABLE OF CONTENTS

ABSTRACT ii

ACKNOWLEDGEMENTS iv

Chapter 1. Introduction 1

Chapter 2. Estimation of Stratocumulus cloud parameters from A-Train observations 6

2.1 Satellite data 6

2.2 Methodology 6

2.2.1 Analyzed stratocumulus clouds 6

2.2.2 Estimation of liquid water path and cloud droplet number concentration 8

2.2.3 Definition of cloud base height 11

2.2.4 Estimation of cloud base rain rate 12

2.3 Retrieval results 14

Chapter 3. Relation among *LWP*, cloud droplet number concentration and cloud base rain rate 22

3.1 Determining factors of warm rain cloud base rain rate 22

3.2 Results 24

Chapter 4. Dependency of auto-conversion rate on cloud droplet number concentration 31

4.1 Dependency of cloud base rain rate on cloud droplet number concentration 31

4.2 Results 32

Chapter 5. Summary and future work 39

References 42

Chapter 1

Introduction

Stratocumulus clouds are convective low-level clouds that develop within the atmospheric boundary layer. They exist broadly where the atmospheric boundary layer is capped by an inversion layer in the subsidence regions of the large-scale circulations such as the Hadley and Walker Circulation in the subtropics, or the baroclinic storm systems and cold-air out breaks in the mid-latitudes (Klein and Hartmann,1993). Regions off the west coast of the continents, such as the northeast Pacific off the coast of California, the southeast Pacific off the coast of Peru, and the southeast Atlantic off the coast of Namibia, are especially well-known for their persistent stratocumulus clouds. The strong inversion layer in these regions are formed by subsidence flow from the subtropical high and low sea surface temperature due to cold currents and coastal upwelling. The relatively low-level stratocumulus clouds tend to reflect much of the incoming solar radiation but have little effect on the outgoing longwave radiation. This leads to a negative radiative forcing effect, and are often referred to as the "air conditioners" of the climate system. Coupled with their persistence, and coverage over large areas, they have a huge impact on the global radiation energy budget and hydrological cycle (Sling, 1990).

It is rare for stratocumulus clouds to produce heavy rainfall, but they do frequently produce light precipitation in the form of drizzle. Subtropical stratocumulus are liquid clouds and their drizzle is produced through warm rain processes. They are driven by convective instability generated from cloud top longwave radiative cooling and surface heat and moisture flux. Drizzle plays an important but complicated role in the formation and maintenance of stratocumulus clouds through its interaction with the vertical profiles of humidity and temperature within the atmospheric boundary layer and the phase changes of the cloud and rain hydrometers (Wood, 2012).

Stratocumulus droplet number concentrations vary as a function of aerosol number concentration. Cloud droplet number concentrations increase with increasing number

concentration of aerosol particles that act as Cloud Condensation Nuclei (Twomey, 1959). Figure 1 shows the estimated cloud droplet number concentrations of maritime stratocumulus clouds globally. Cloud droplet number concentrations are high near the coast (particularly the western coasts) and low in remote oceans, varying from $10\ cm^{-3}$ in pristine environment to more than $500\ cm^{-3}$ in polluted regions (e.g. Wood, 2012). The fact that coastal waters off the west coast of subtropical continents are persistently covered by stratocumulus clouds makes these regions an ideal testbed for studying cloud physical and dynamical processes of warm rain clouds.

Numerous observational as well as modelling studies have been used to investigate the relation between rain rate and cloud droplet number concentration in stratocumulus clouds from the viewpoint of the impact of the change in background aerosol on precipitation efficiency, spatial distribution and lifetime of cloud system via its ability to modulate cloud droplet number concentration. This effect, referred to as the second aerosol indirect effect, was first proposed by Albrecht (1989). He showed using simple model simulations that higher CCN could increase the longevity and optical thickness of stratocumulus clouds. He hypothesized that higher CCN concentrations could decrease the cloud droplet size, thereby reducing the collision-coalescence efficiency of cloud droplets which, in turn, could lead to the suppression of rainfall (and less removal of cloud water) and result in the increase of both cloud water and life time. Jiang et al. (2002) confirmed that higher CCN could suppress the cloud base rain rate from the simulation of Atlantic stratocumulus utilizing a more sophisticated model that employed a detailed cloud microphysics scheme. However, they also found that suppressed rainfall would lead to a smaller *LWP* caused by the stabilization of the atmospheric boundary layer that resulted from reduced evaporative cooling. The effect of aerosols on the spatial distribution and longevity of stratocumulus clouds differs amongst studies, but most of them found a common behavior in that higher CCN suppressed rainfall. Wood (2005) showed that cloud base rain rate in stratocumulus clouds decreases with higher cloud droplet number concentrations by utilizing observational data collected by aircraft in-situ measurements and ground-based remote sensing from seven different field campaigns. Leon et al. (2008) found similar trends from CloudSat observations. Various

modeling studies, including those utilizing Large-eddy-simulation (LES; e.g. Ackerman et al.,2008) and cloud resolving model simulation（e.g. Wang et al.,2011), also suggest that cloud base rain rates of stratocumulus clouds decrease with higher cloud droplet number concentration. Many studies have found that cloud base rain rate (R_{cb}) not only weakens with increasing cloud droplet number, but also intensifies with increasing cloud thickness, *H*, or *LWP*. For stratocumulus clouds off the coast of Peru, Comstock et al. (2004) derived an empirical relation $R_{cb} \propto \left({LWP}/{N_d}\right)^{1.75}$ from shipborne observations consisting of radar, pyranometer and microwave radiometer data. Vanzanten et al. (2005) proposed a slightly different relation $R_{cb} \propto {H^3}/{N_d}$ from aircraft in-situ observations off the coast of California. Geoffroy et al. (2008) showed that LES simulations reproduced relations among cloud base rain rate, cloud droplet number concentration and *LWP* which were consistent with those proposed by Comstock et al. (2004) and Vanzanten et al. (2005), concluding that the empirical relations derived from observation have a physical basis.

The precipitation process within warm stratocumulus clouds is relatively well understood. Precipitation particles begin to grow by collision-coalescence and become raindrop embryos through the process referred to as auto-conversion. Raindrop embryos continue to grow in size and start to fall once they become too large to be supported by the updraft. While falling through the cloud layer, rain drops keep growing by collecting cloud droplets until they reach the cloud base through the process of accretion. The parametrization of this auto-conversion process can generally be written as a power law of the liquid water content (LWC) and cloud droplet number concentration near the cloud top (Liu and Daum, 2004). Assuming a continuous collection model for the accretion growth of raindrops, cloud base rain rate is determined mainly by the *LWP* and cloud droplet number concentration as seen above. Abel et al. (2010) investigated the relation between cloud base rain rate and *LWP* for stratocumulus clouds over the southeast Pacific, simulated by the United Kingdom's Meteorological Office Unified Model with a one-moment cloud scheme. They found that the results of their simulation best fit the empirical relation proposed by Comstock et al. (2004) when assuming cloud droplet number concentrations of $63\ cm^{-3}$. Because the simulations were actually utilizing an assumed cloud droplet number

concentration of $100\ cm^{-3}$, they suggested that auto-conversion rate of the Unified Model was producing rain too efficiently.

The relation among R_{cb}, LWP and cloud droplet number concentration provides useful information not only for an enhanced theoretical understanding of the mechanisms of stratocumulus formation, but also for the parametrization of precipitation processes in numerical weather models. However, the limited field campaign domains, and the relatively small amounts of data available in previous studies, makes it difficult to draw statically significant conclusions regarding these processes, or to make globally applicable inferences.

The aim of this study is to obtain statistically robust relations among liquid water path, cloud droplet number concentrations and cloud base rain rates for three geographical regions with similar environments, namely the northeast Pacific off the coast of California, the southeast Pacific off the coast of Peru and the southeast Atlantic off the coast of Namibia, by utilizing space-borne observation from the A-Train satellites. Sensitivity of both the auto-conversion rates and cloud base rain rates to the cloud droplet number concentration is also assessed from numerous satellite observations.

Chapter 2 describes the data and methodology used to estimate cloud parameters from A-Train satellite observations. Chapter 3 presents the relation obtained from satellite observation and compares them with those of previous studies. Inter-comparisons among the three study regions is also presented. Chapter 4 discusses the sensitivity of auto-conversion rate to cloud droplet number concentration based on the relation between cloud base rain rate and cloud droplet number concentration. Conclusions from this study are given in Chapter 5.

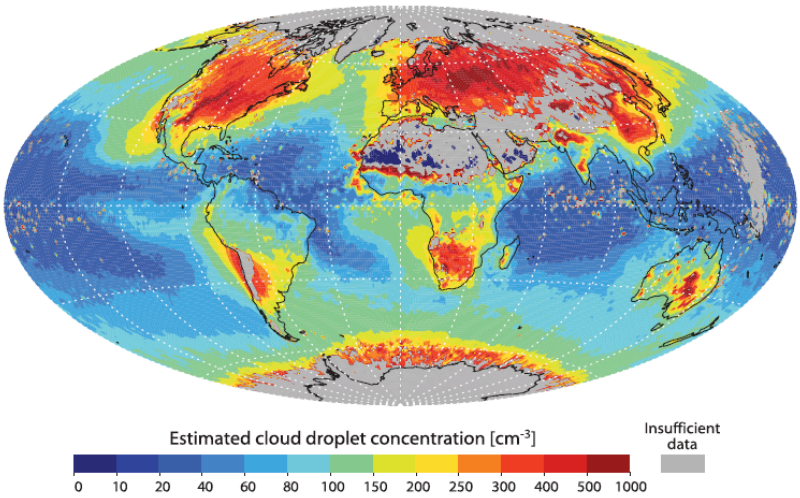

Fig. 1.1. Global distribution of cloud droplet number concentration for stratocumulus clouds estimated from MODIS observations (after Figure.23 of Wood (2012)).

Chapter 2

Estimation of Stratocumulus cloud parameters from A-Train observations

2.1 Satellite data

Satellite observations from CloudSat's Cloud Profiling Radar (CPR) (Stephens et al, 2002), CALIPSO's spaceborne lidar (Winker et al., 2003) and Aqua's Moderate Resolution Imaging Spectroradiometer (MODIS) (Parkinson, 2003), all of which fly in the A-Train, are used for estimating cloud parameters in this study. All of the data are matched up to CloudSat footprints. The horizontal and vertical resolutions of CloudSat observations are approximately 1.75km and 240m respectively. Cloud base geometrical height and rain rates are estimated from the radar reflectivity profile through the 2B-GEOPROF product (Marchand et al., 2008) described later. Cloud top geometrical height and cloud layers are derived from the 2B-GEOPROF-LIDAR product (Mace and Zhang, 2014). It is difficult for the radar to detect thin clouds. The 2B-GEOPROF-LIDAR product improves the detection of such clouds by combining radar and lidar observation. Cloud optical thickness and cloud effective radius are derived from the MOD06-1KM-AUX product which is a subset of MODIS Collection 6 cloud product matched to the closest CloudSat footprints. Temperature and pressure data from ECMWF-AUX product are used as auxiliary data. The ECMWF-AUX product is a set of ECMWF state variable data interpolated to each CloudSat bin.

2.2 Methodology

2.2.1 Analyzed stratocumulus clouds

Subtropical maritime warm stratocumulus clouds off the west coast of various continents are analyzed in this study. Data for three years from 2008 to 2010 are used for the analysis. This period was chosen so as to include campaign period of VAMOS Ocean-Cloud-Atmosphere-Land Study Regional Experiment (VOCALS-Rex) (Wood et al,2011). Satellites flying on the A-train orbit observe each location on the globe twice a day both day and night. Only daytime observations

(around 13:30 local time) are analyzed in this study because MODIS visible bands require visible reflectance that is available only during daytime.

In this study, stratocumulus clouds are defined as single-layer low-level clouds existing in the northeast Pacific, the southeast Pacific or the south east Atlantic (Table 2.1), whose cloud top height and temperature are below 3000m and above 268K respectively. The definition of the study regions is adopted from the previous study on the climatology of stratocumulus clouds (Muhlbauer et al., 2014). Under the subsidence regimes of the subtropical highs, mid- and upper-level cloud development are typically suppressed. The analysis was limited to single-layer clouds so as to select typical environments for the development of subtropical stratocumulus clouds. The International Cloud Climatology Project (ISCCP; Rossow and Schiffer, 1991) defines low clouds by cloud top pressures of less than 680hPa, or maximum cloud top geometric heights of 3000m corresponding to 680 hPa in pressure coordinate. Aiming to select only liquid-phase clouds, minimum cloud top temperature is set to 268K based on the criteria used in a previous study on estimating cloud droplet number concentration of stratocumulus clouds (Bennartz and Rausch, 2017).

Figure 2.1 shows the frequency of occurrence of low clouds observed by CloudSat / CALIPSO. Regions enclosed by red lines denote the selected analysis domains of this study. The upper panel shows the occurrence of low clouds including those that are overlapped by higher clouds, while the lower panel shows the occurrence of single layer low clouds only. The frequent occurrence of low clouds in the subtropical oceans off the west coast of continents (the subject of this study), as well as the mid-latitude storm tracks, are clearly evident in this figure. Low clouds found in the former regions tend to be more single-layered compared to those in the latter regions. This difference is likely the result of the different large-scale environments driving these systems.

Figure 2.2 shows a scatter diagram of cloud top temperature and height of the lowest clouds for the 3 regions analyzed in this study. The left panels show results from single-layer clouds while the right panels show results of multiple-layer clouds. All three regions show that the occurrence of single-layer low clouds is one order of magnitude larger than that of low clouds with overlapped

clouds. Clouds with top heights of less than 3000 m are mostly liquid-phase clouds in the analysis regions in this study as determined from ERA5. However, there are significant numbers of mixed-phase clouds whose cloud top heights are less than 3000 m. Cloud top temperature is therefore adopted as a secondary threshold for selecting liquid-phase cloud in these regions.

2.2.2 Estimation of liquid water path and cloud droplet number concentration

LWP and cloud droplet number concentrations are calculated from optical depth and effective radius provided by the MODIS collection 6 cloud product (Platnick et al., 2017). These quantities are estimated assuming that 1) cloud are horizontally homogeneous, 2) cloud liquid water content (LWC) increases monotonically within the cloud layer, and 3) cloud droplet number concentrations are vertically constant within the cloud layer. Many in-situ observation and modeling studies (e.g., Nicholls and Leighton 1986; Brenguier et al. 2000; Wood 2005; Klein et al.2009) show that these assumptions are generally valid for stratocumulus clouds. In this sub-section, equations for estimating cloud liquid water path and cloud droplet number concentration are derived following Grosvenor et al. (2018).

Assuming a spherical cloud droplet, cloud optical thickness τ is defined using Eq. (2.1):

$$\tau = \int_0^H \beta_{ext}(z)dz \tag{2.1}$$

$$\beta_{ext}(z) = \pi \int_0^\infty Q_{ext}(r)\, r^2 n(r) dr \tag{2.2}$$

where $\beta_{ext}(m^{-1})$ is the cloud extinction coefficient given by Eq. (2.2), $Q_{ext}(r)$ is the unitless extinction efficiency factor, $n(r)(m^{-4})$ is droplet number size distribution, and $H(m)$ is cloud geometrical thickness. Since wavelengths of MODIS visible and near-infrared bands are short compared to cloud droplet diameters, the Geometric optics approximation holds in these wavelengths. Thus, $Q_{ext}(r)$ can be approximated as $Q_{ext}(r) = Q_{ext} = 2$. Following the same notation, droplet number concentration $N_d(z)(m^{-3})$, droplet effective radius $r_e(z)(m)$ (Hansen and Trivas,1974) and volume-mean droplet radius are defined as Eq. (2.3), (2.4) and (2.5)

respectively. We also introduce the "k" value which relates volume-mean droplet radius to droplet effective radius as Eq. (2.6):

$$N_d(z) = \int_0^\infty n(r)dr \tag{2.3}$$

$$r_e(z) = \frac{\int_0^\infty r^3 n(r)dr}{\int_0^\infty r^2 n(r)dr} \tag{2.4}$$

$$r_v{}^3(z) = \frac{1}{N_d(z)} \int_0^\infty r^3 n(r)dr \tag{2.5}$$

$$k = \left(\frac{r_v(z)}{r_e(z)}\right)^3 \tag{2.6}$$

The relation between cloud liquid water content $\mathrm{L}(z)(kgm^{-3})$ and cloud droplet number concentration is generally expressed in the form of Eq. (7), where $\rho_w(kgm^{-3})$ is density of water.

$$\mathrm{L}(z) = \frac{4\pi\rho_w}{3} \int_0^\infty n(r) r^3(r)dr \tag{2.7}$$

Combining Eq. (2.5), (2.6) and (2.7) gives Eq. (2.8), which expresses the droplet effective radius as a function of cloud liquid water content and cloud droplet number concentration:

$$k r_e{}^3(z) = \frac{3L(z)}{4\pi\rho_w N_d(z)} \tag{2.8}$$

Combining Eq. (2.2), (2.4) and (2.6) gives Eq. (2.9) which now expresses the cloud extinction coefficient as a function of cloud liquid water content and cloud effective radius:

$$\beta_{ext}(z) = \frac{3Q_{ext}L(z)}{4\rho_w r_e(z)} \tag{2.9}$$

Since we assume cloud liquid water content increases monotonically toward cloud top within the cloud layer, the liquid water content $\mathrm{L}(z)$ and liquid water path $\mathrm{L}WP$ can be written as Eq. (2.10) and (2.11) respectively:

$$\mathrm{L}(z) = f_{ad} c_w z \tag{2.10}$$

$$LWP = \frac{1}{2} f_{ad} c_w H^2 \tag{2.11}$$

where $c_w(kgm^{-4})$ is the adiabatic condensate rate and f_{ad} is the unitless adiabaticity factor.

Under the assumption that cloud droplet number concentration is vertically constant within the cloud layer ($N_d(z) = N_d$), combining and rearranging Eq. (2.8), (2.9), (2.10) and substituting into Eq. (2.1) gives Eq. (2.12):

$$\tau = \frac{3Q_{ext}}{5}\left(\frac{3f_{ad}c_w}{4\rho_w}\right)^{2/3}(N_d\pi k)^{1/3}H^{5/3} \tag{2.12}$$

Letting $z = H$, solving Eq. (9) and (10) for H, and substituting into Eq. (2.12), cloud droplet number concentration N_d can be expressed as Eq. (2.13):

$$N_d = \frac{\sqrt{5}}{2\pi k}\left(\frac{f_{ad}c_w\tau}{Q_{ext}\rho_w {r_e}^5}\right)^{1/2} \tag{2.13}$$

Similarly, letting $z = H$, solving Eq. (2.9) and (2.10) for N_d, substituting into Eq. (2.12), and eliminating $f_{ad}c_w$ by using Eq. (2.12), the liquid water path, LWP, can be expressed as Eq. (2.14):

$$LWP = \frac{10}{9Q_{ext}}\rho_w\tau r_e(H) = \frac{5}{9}\rho_w\tau r_e(H) \tag{2.14}$$

The MODIS cloud product provides effective radius at $1.6\mu m$, $2.1\mu m$ and $3.7\mu m$. Studies have suggested that cloud effective radius at $3.7\mu m$ ($r_{e,3.7}$) is less prone to pixel heterogeneity compared to the other two (Grosvenor et al, 2018). It is therefore used as the cloud effective radius near cloud top in this study. Adiabatic condensate rate c_w is calculated from the cloud base pressure and temperature obtained from ERA5 with the assumption that c_w is vertically constant within the cloud layer. Cloud base is determined by the CloudSat radar profile.

Based on the results of aircraft observations (Martin et al., 1994; Pawlowska and Breguier, 2003), the "k" value is set as 0.8. Adiabaticity is set as 1, which follows previous studies for estimating cloud droplet number concentration from MODIS observations that assume condensation rates to be completely adiabatic (e.g. Bennartz, 2007). It is known from aircraft observations that adiabaticity in stratocumulus varies largely from 0.1 to 0.9 (Albrecht et al., 1985; Boers et al., 1998; Brenguier et al., 2000; Ishizaka et al., 1995; Min et al., 2012; Nicholls & Leighton, 1986; Painemal and Zuidema, 2011; Rogers and Telford, 1986). Since we are only

analyzing daytime stratocumulus clouds within subsidence regions, these clouds are likely to have similar large values. Also, the value of adiabaticity contributes to the estimated number concentration by power of one-half. Setting adiabaticity to 1 therefore appears to be a reasonable first-order approximation.

Droplet number concentration and *LWP* are calculated only for those pixels whose optical thickness exceeds 5 and effective radius satisfies $r_{e,3.7} > r_{e,2.1} > r_{e,1.6}$. The former criterion is for excluding thin clouds typically have larger estimation errors for their effective radius due to its sensitivity to reflectance. The latter is for extracting relatively homogeneous pixels, which also satisfy our cloud assumption that liquid water content monotonically increases with height within the cloud layer.

2.2.3 Definition of cloud base height

Cloud base is defined from the vertical profile of the CloudSat radar reflectivity. Previous observational studies suggested that radar reflectivity reaches its maximum around cloud base (Wood, 2005; vanZanten et al., 2005). This is consistent with our theoretical understanding of precipitation processes that rain embryos formed near the cloud top grow by collecting cloud droplets while falling through the cloud layer but contract once below cloud base due to evaporation. Cloud base is defined as the radar bin that has the largest reflectivity among the bins between the fifth bin from the surface (i.e.960m from the surface) and cloud top identified in 2B-GEOPROF-LIDAR product, after correcting for water vapor attenuation using the value provided in 2B-GEOPROF product. CloudSat operates at a frequency of 94GHz which is heavily affected by attenuation due to water vapor and hydrometeors. It is assumed that the vertical change of total attenuation of cloud droplets is much smaller than that of water vapor near cloud base.

Radar reflectivity data of the nearest 4 bins from the surface are excluded from our analysis because these bins are heavily contaminated by surface clutter (Marchand et al., 2008). This treatment will lead to the overestimation of cloud base height, especially in the case when the actual cloud base is below 1km. However, from the following physical consideration and

observational results, we assume that the effect of this treatment on the estimated cloud base radar reflectivity is very small. From the cloud physics point of view, it is assumed that raindrops, which are the dominant contributor to the increase of radar reflectivity, will grow very slowly near cloud base since both liquid water content and collection efficiency are small. In fact, previous studies using ground-based radar observation of stratocumulus clouds found that the radar reflectivity increases rapidly near cloud top and remains fairly constant near cloud base (Comstock et al.,2004).

Figure 2.3 shows the probability density distributions of cloud base radar reflectivity estimated from the algorithm used in this study and from a slightly different algorithm which includes an additional bin closer to the surface (the fourth bin from the surface). Overall, the probability density distributions are similar, which suggests that the effect of overestimating cloud base height on the estimated cloud base reflectivity is small. However, if the fourth bin from the surface is allowed in this analysis, there is a peak around $-15\ dBZ$ which is not found when this bin is removed. Figure 2.4 shows the estimated surface clutter profile for CloudSat. It can be seen that the peak around $-15\ dBZ$ in Figure 2.3 corresponds to the surface clutter at the fourth bin from the surface, suggesting that using this bin in the current study would heavily affect the estimated cloud base radar reflectivity. The fourth bin is therefore excluded from the analysis.

2.2.4 Estimation of cloud base rain rate

The precipitation of stratocumulus clouds is generally weak and thus evaporation of raindrops in the sub-cloud layer is not negligible. Since our interest is in the precipitation formation of stratocumulus clouds, we focus specifically on the rain rate at cloud base which is considered to be the strongest in the column. A Z-R relation is employed to estimate R_{cb} from radar reflectivity observed by CloudSat. In order to take into account the variability of rain/drizzle/cloud droplets size distribution of stratocumulus clouds, rain rate is calculated as the mean of those derived from five different Z-R relations which are presented in previous aircraft and ground-based observational studies. Maximum and minimum values obtained from the five different Z-R relations are assigned to an estimation error.

Figure 2.5 shows the Z-R relations employed in this study as well as the five relations presented in the previous studies. Table 2.2 shows the observation area and method, as well as parameters of each Z-R relation for each five relations used in this study. These relations were obtained from ground-based radar and aircraft observation of southeast Pacific stratocumulus clouds from the East Pacific Investigation of Climate (EPIC) field campaign (Comstock et al., 2004) and aircraft observation of northeast Atlantic stratocumulus clouds (Wood, 2005). We expect that the inclusion of the Z-R relations derived in the northeast Atlantic, which is outside of our interest in this study, will incorporate a wide range in the droplet size distributions due to their different environments outside of subtropical subsidence regions. To account for the disproportionate impact of large drops which in-situ aircraft observations often underestimate, we employed two types of Z-R relations derived from aircraft observation. The first uses an extrapolated droplet size distribution assuming an exponential shape and the second without extrapolation.

Z-R relations are applied to radar reflectivity data corrected for water vapor and cloud droplet attenuation and temperature dependency of the index of refraction. The correction for water vapor attenuation is employed from the 2B-GEOPROF product which is same as the case in determining cloud base height. Eq. (2.15), which was proposed by Liebe et al. (1989) is employed to correct for cloud droplets attenuation:

$$\alpha = \mathrm{La}\theta^{b} \tag{2.15}$$

Here, α is the cloud droplet attenuation (dB/km), θ is defined as $\theta = {}^{300}/_{T_{cb}}$ where $T_{cb}(K)$ is cloud base air temperature, $a = 3.73$ and $\mathrm{b} = 2.81$. It is worth noting that Eq. (2.15) was found to be valid for airborne W-band radar observation of stratocumulus clouds (Vali and Haimov, 2001), because the frequency is same as that of CloudSat.

The valid radar reflectivity range for applying these Z-R relations is determined from the reflectivity range used for obtaining those relations. It is considered that rain rate estimation from Z-R relations is quantitatively valid for radar reflectivity ranging between $-25\ dBZ$ to $10\ dBZ$.

Uncertainties due to the difference in Z-R relations are also assigned to this range. For those data outside of this range, it is considered that the estimated rain rate is only qualitatively valid and estimation uncertainties are not evaluated.

2.3 Retrieval results

The characteristics of our estimated cloud base rain rate, *LWP*, and cloud droplet number concentration for Californian (NEP), Peruvian (SEP) and Namibian (SEA) stratocumulus clouds are explored. Cloud top height serves as a good indicator for the thickness of the atmospheric boundary layer in these three regions since they are determined mainly by the strength of the subsidence flow from the subtropical high, and hence by the corresponding inversion layer. Figure 2.6 shows the regional probability density function of cloud top height, cloud droplet number concentration, *LWP* and cloud base of the data that pass the quality control processes described in this section. While the atmospheric boundary layer seems to be slightly deeper at NEP, as suggested from the fact that peak of the cloud top height is higher at NEP compared to those of SEP and SEA (Figure 2.6(a)), the peaks are located at around 1500 m for all three regions. We therefore assume that there is no significant difference among analyzed clouds from the three different regions in terms of their dynamical and thermodynamical environment. It is also noted that, due to the exclusion of optically thin clouds, clouds with top heights of less than 1000 m are not analyzed in this study.

LWP is distributed broadly from less than $20\,\mathrm{g}\,m^{-2}$ to more than $300\,\mathrm{g}\,m^{-2}$ with a maximum frequency value located around $70\,\mathrm{g}\,m^{-2}$ for all three regions (Figure 2.6(c)). NEP has a tendency for larger *LWP* compared to the other two regions. Cloud droplet number concentrations (Figure 2.6(b)) are also broadly distributed and range from less than $10\,cm^{-3}$ to more than $300\,cm^{-3}$ for all three regions. NEP tends to have larger cloud droplet number concentration with its maximum frequency value found around $80\,cm^{-3}$, whereas those for SEP and SEA are found around $60\,cm^{-3}$. The distribution of radar reflectivity (Figure 2.6(d)) is nearly the same for all three regions. The majority of the observations have radar reflectivity of less than

$-20\ dBZ$, suggesting light- or non-precipitating clouds. Heavily precipitating clouds with radar reflectivity exceeding $10\ dBZ$ are not present, which is in keeping with our theoretical expectations of stratocumulus precipitation rates.

In summary, the methodology used in this study successfully samples stratocumulus clouds with light or no precipitation in various locations and thermodynamic environments in terms of their cloud droplet number concentration and *LWP*. Although the distributions of *LWP* and cloud droplet number concentration, which are the main factors for determining stratocumulus cloud base rain rate, are slightly different at NEP compared to the other two regions, the distribution of radar reflectivity is nearly the same for all three regions. We speculate that this is due to the offset of precipitation suppression by the high cloud droplet number concentrations and enhancement of rain formation by large *LWP*.

Table 2.1 Analyzed regions and their location.

Region	Domain
Northeast Pacific (NEP)	15–35N, 120–140W
Southeast Pacific (SEP)	10–30S, 75–95W
Southeast Atlantic (SEA)	10–30S, 10W–10E

Table 2.2 Area and method of observation and derived Z-R relations in previous studies. a and b are parameters defining Z-R relation where $Z = aR^b$.

Region	Observation method	a	b
Northeast Atlantic(Wood,2005)	Aircraft（with extrapolation）	6.0	1.04
	Aircraft（w/o extrapolation）	12.4	1.18
Southeast Pacific (Comstock,2004)	Aircraft（with extrapolation）	22	1.1
	Aircraft（w/o extrapolation）	32	1.4
	Ground-based radar	25	1.3

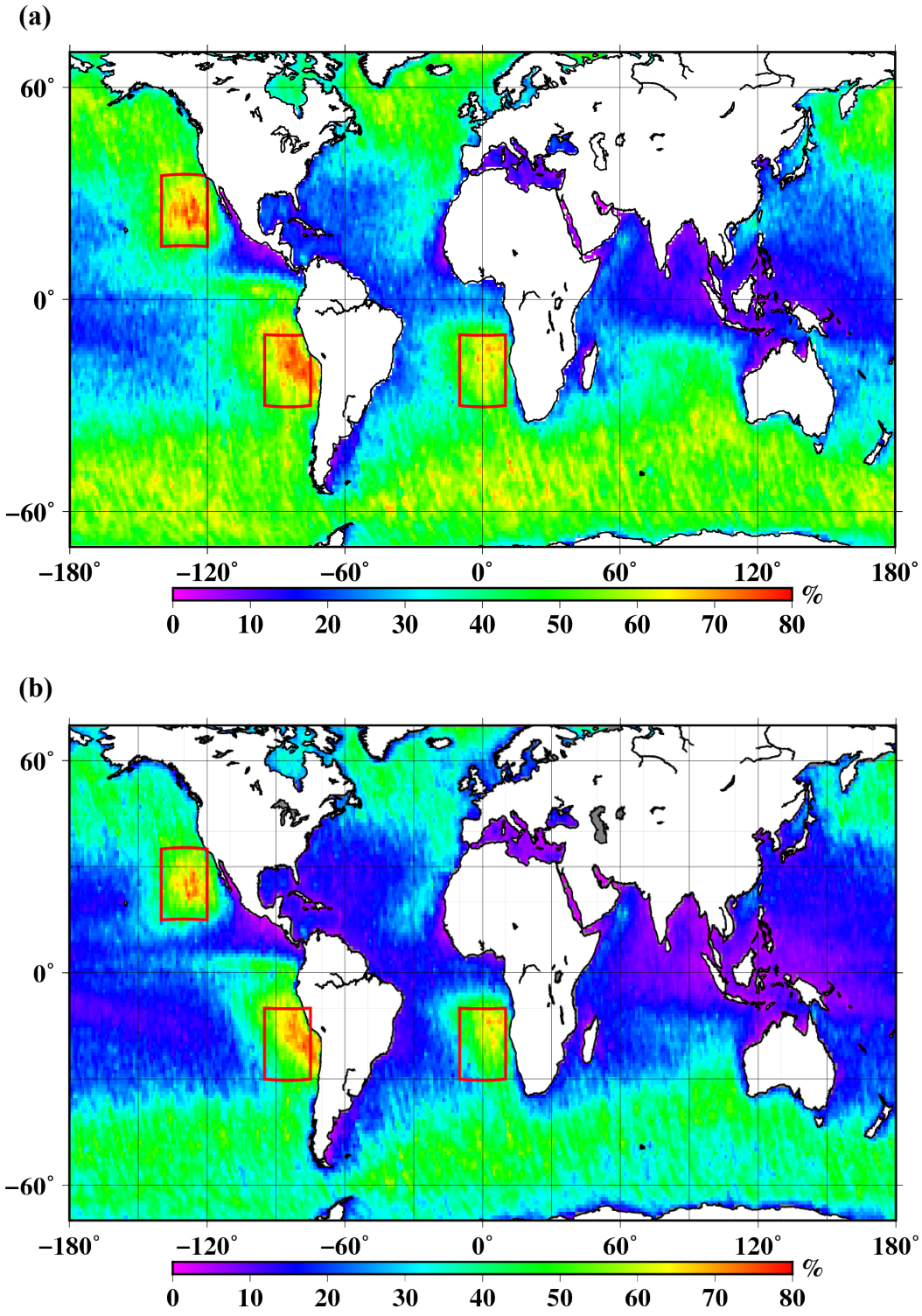

Figure 2.1 Occurrence frequency of low clouds observed by CloudSat/CALIPSO observation for (a) those overlapped by higher clouds and for (b) single-layer clouds only. Regions enclosed by red lines demote the analysis areas in this study. Data period is three years from 2008 to 2010. Observation is made at daytime (approx.13:30) in local time.

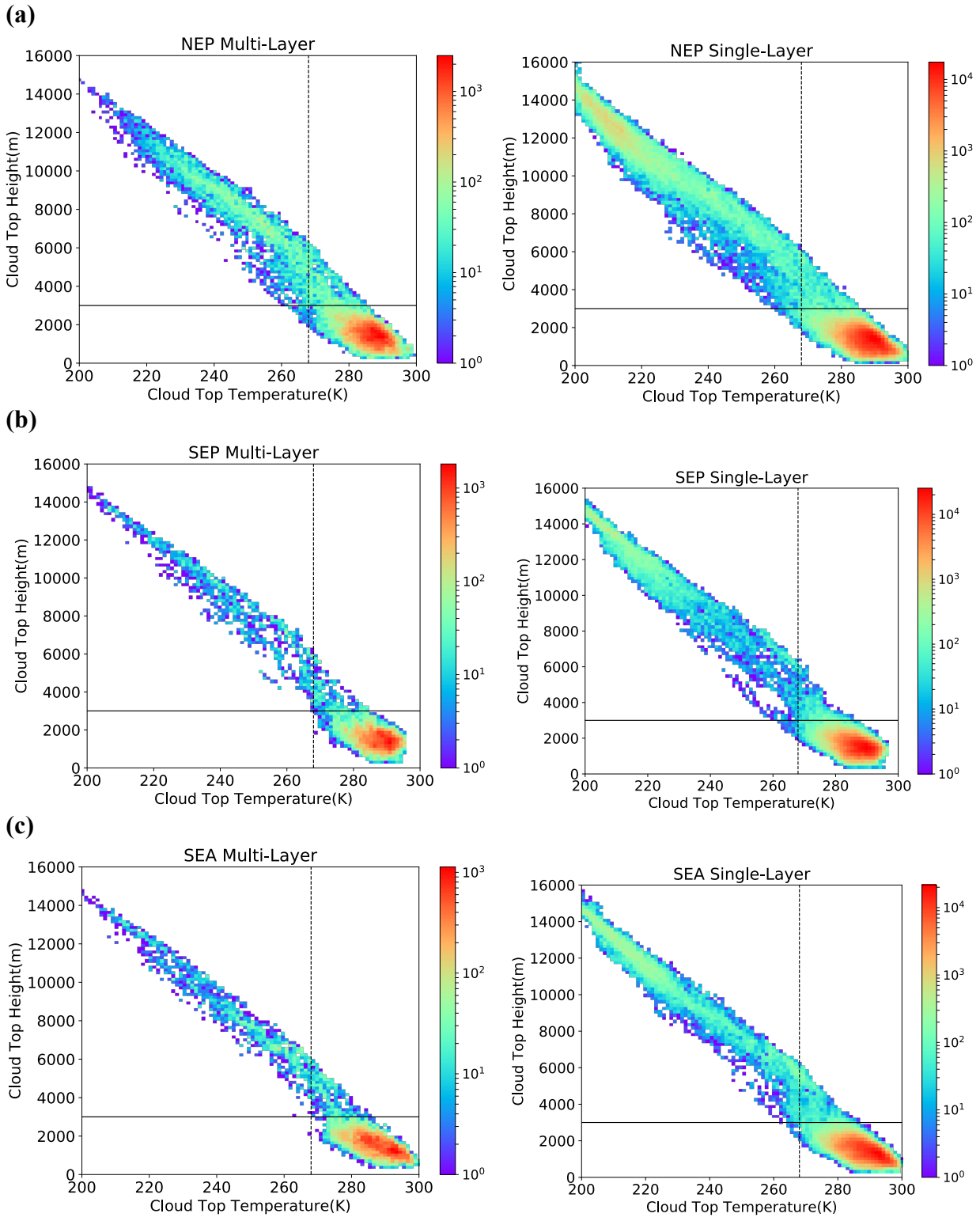

Figure 2.2 Scatter diagrams of cloud top temperature and height of lowest clouds for (a) NEP, (b) SEP and (c) SEA. Low clouds are divided into single layer cloud (left panels) and multi-layer clouds (right). Stratocumulus is defined as cloud with cloud top height below 3000m (solid line) and cloud top temperature above 268K (dashed line)

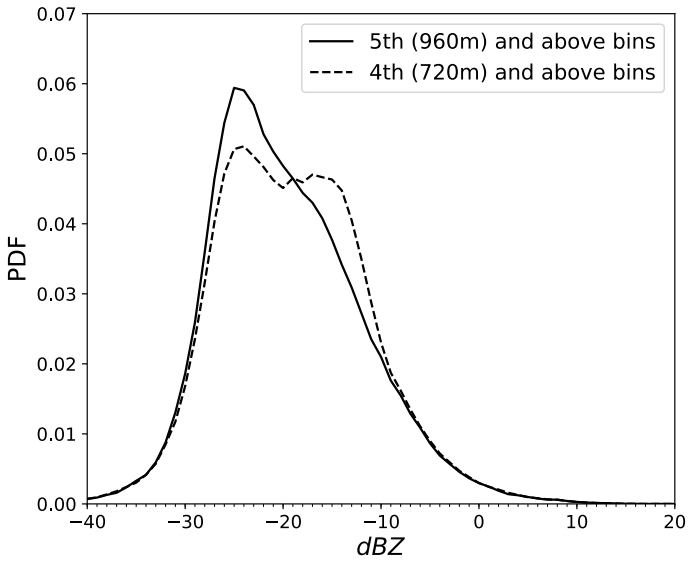

Figure 2.3 Probability density distributions of estimated cloud base radar reflectivity by utilizing bins above and include the 5th bin (solid line) and 4th bin (dashed line), respectively. The former adopts the same assumption as employed in this study.

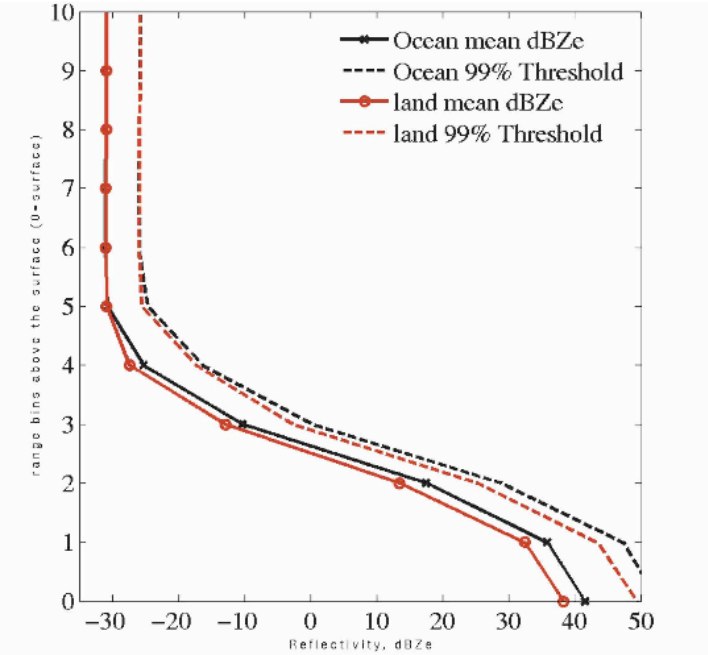

Figure 2.4 Estimated surface clutter profile for CloudSat. Shown is the mean for maritime scenes (black solid line) and land scenes (red solid line). 99% confidence intervals are denoted with dashed lines (after Fig 7 of Marchand et al. (2007)).

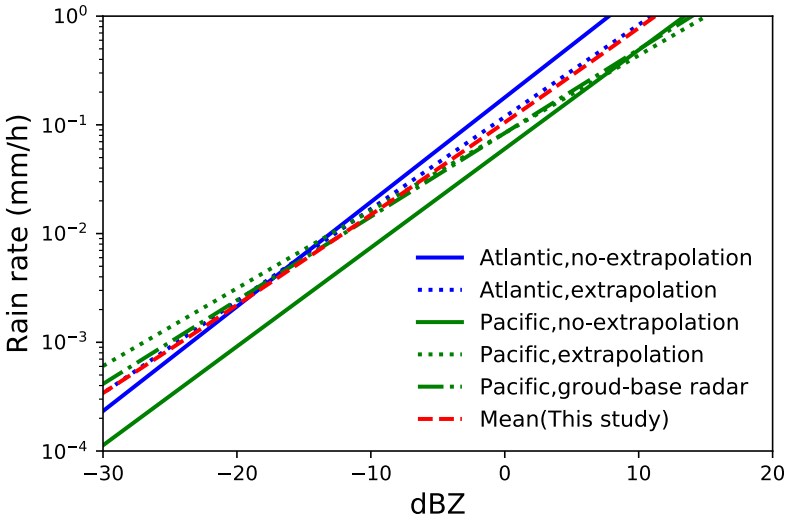

Figure 2.5 Z-R relation employed in this study and those from five previous studies. Atlantic and Pacific Z-R relations are obtained from aircraft observation of northeast Atlantic stratocumulus clouds (Wood, 2005), ground-based radar and aircraft observation of southeast Pacific stratocumulus clouds from the East Pacific Investigation of Climate (EPIC) field campaign (Comstock et al., 2004) respectively.

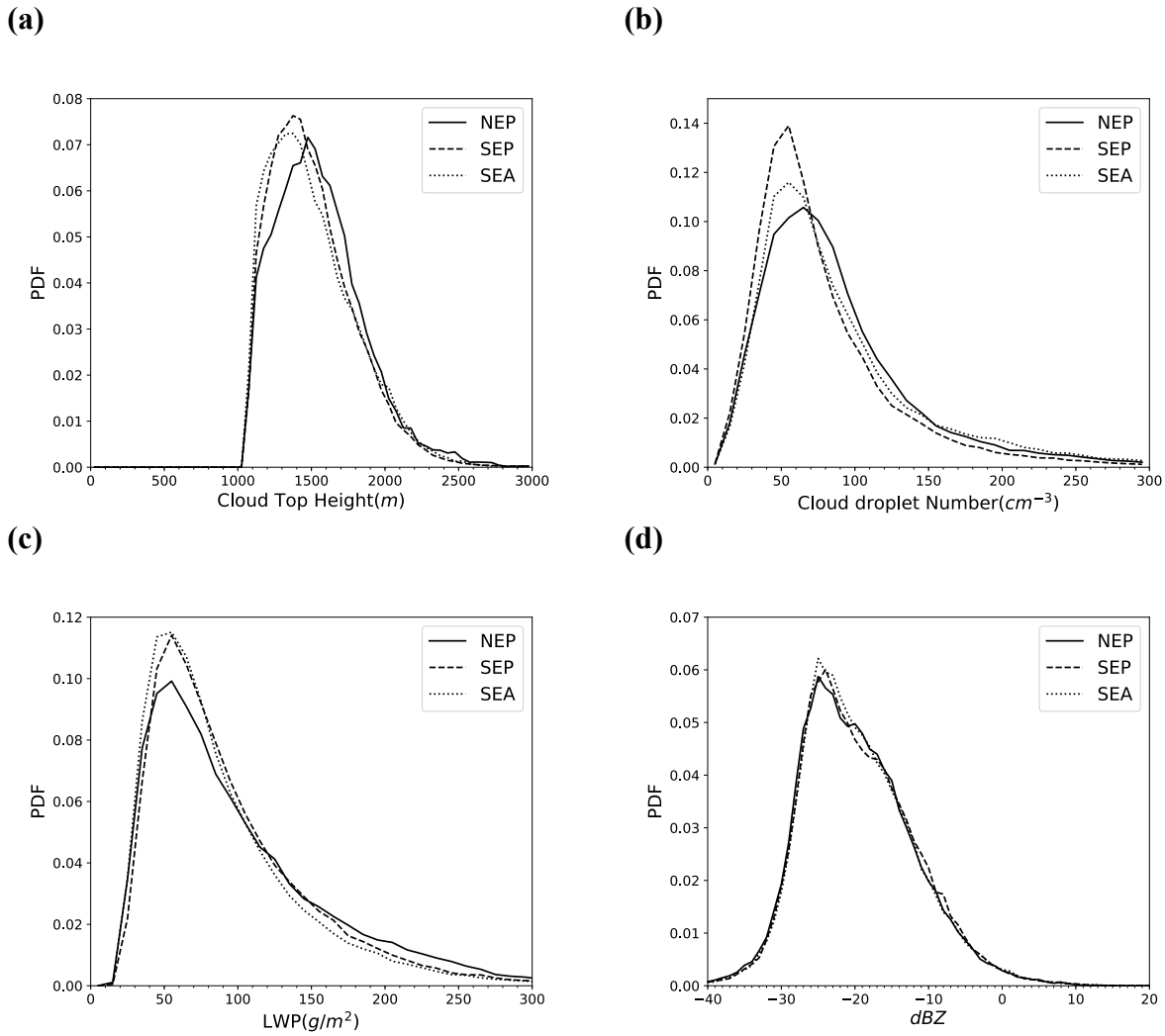

Figure 2.6 Probability density functions of (a) cloud top height, (b) cloud droplet number concentration,(c) *LWP* and (d) cloud base radar reflectivity for NEP (Solid lines), SEP (dotted lines) and SEA (dashed lines).

Chapter 3

Relation among *LWP*, cloud droplet number concentration and cloud base rain rate

3.1 Determining factors of warm rain cloud base rain rate

Precipitation particles observed at the cloud base of a warm cloud are formed through conversion of cloud droplets to raindrop embryos (auto-conversion), followed by growth of those rain embryos through the collection of cloud droplets as they fall through the cloud layer. Since these processes are modulated by cloud droplet number concentration and *LWP*, the relation between these parameters and cloud base rain rate contains information on auto-conversion and accretion. As we are only analyzing those stratocumulus clouds developing in similar environments, we assumed that the following two approximations are valid. First, that LWC is a monotonic function of LWP, which is derived from the assumptions of constant moist adiabatic lapse rate and monotonic increase of liquid water content within the cloud layer. The second is that rain drops from clouds with similar *LWP* will sweep out similar amounts of liquid water until they reach cloud base. This is derived from the initial assumption that vertical motion is the same for all clouds. Based on these approximations, we qualitatively discuss the impact of auto-conversion on the relation among cloud droplet number concentration and *LWP*.

Auto-conversion rate (P) is determined by the size distribution and collision-coalescence efficiency of cloud droplets. Many parameterizations have been proposed with different assumptions on the cloud droplet size distributions (e.g. Berry and Reinhardt, 1974; Khairoutdinov and Kogan, 2000). These schemes can be expressed by the following general formula, where $H(y - y_c)$ is the Heaviside Step function:

$$P \propto LWC^{\alpha} N_d^{-\beta} H(y - y_c) \tag{3.1}$$

Typically, y and y_c are a function of cloud droplet sizes. Eq. (3.1) implies that cloud droplets should be larger than a certain size for the activation of auto-conversion. It also implies that, at a given cloud droplet number concentration, higher *LWC (LWP)* near cloud top will enhance the

conversion of cloud droplets to raindrop embryos by enhanced collision-coalescence efficiency due to larger cloud droplet sizes, whereas higher cloud droplet number concentration will suppress the auto-conversion, by effectively reducing cloud droplet sizes.

Raindrop embryos produced by auto-conversion will grow and eventually become raindrops by collecting cloud droplets while they fall through the cloud layer. Assuming a continuous collection growth model, the growth rate of raindrops is written as Eq. (3.2):

$$dr_d \propto \overline{K(r_d, r_c)} LWP \tag{3.2}$$

where dr_d is the change in the radius of raindrops between cloud top and bottom, and $\overline{K(r_d, r_c)}$ is the cloud layer mean accretion efficiency of rain and cloud droplets. Accretion efficiency is generally a function of the diameters of the raindrop (collector) and the cloud droplet (collected), and generally has a higher efficiency for larger cloud droplets. Assuming that raindrop embryos produced from auto-conversion have the same size, $\overline{K(r_d, r_c)}$ becomes a function of cloud droplets size. Combining this with the fact that cloud droplet size is a function of LWC and cloud droplet number concentration, Eq. (3.2) becomes a function of LWP and cloud droplet number concentration. Eq. (3.2) thus implies that the growth rate of raindrops becomes larger with fewer cloud droplet number concentration and larger LWP.

Larger cloud droplet sizes and enhanced raindrop embryo production near the cloud top will intensify the cloud base rain rate R_{cb}. Since the cloud droplet size and number concentration of raindrop embryos produced by auto-conversion both increase with larger *LWP* and fewer cloud droplet number concentration, cloud base rain rate R_{cb} will be intensified by increase of LWP and decrease of cloud droplet number concentration. Therefore, if the model tends to simulate stronger (weaker) cloud base rain rates compared to the observation of clouds with the same droplet number concentration and *LWP,* we could infer that model representation of auto-conversion or accretion growth is over- (under-) estimated.

As summarized in Geoffroy et al.(2008), a number of empirical formulae have been proposed from different observations for the relation among *LWP*, cloud droplet number

concentration and cloud base rain rate, such as $R_{cb} \propto {LWP^2}/{N_d}$ from the 2nd Aerosol Characterization Experiment (ACE-2) (Raes et al., 2000), $R_{cb} \propto \left({LWP}/{N_d}\right)^{1.75}$ from the EPIC (Bretherton et al., 2004) and $R_{cb} \propto {LWP^{1.5}}/{N_d}$ from the Dynamics and Chemistry of Marine Stratocumulus cloud experiment (DYCOM-II) (Stevens et al., 2003) . In this study, we employed the empirical relation obtained from EPIC filed campaign $R_{cb} \propto \left({LWP}/{N_d}\right)^{1.75}$ (Comstock et al., 2004) as a baseline.

3.2 Results

Figure 3.1 shows the probability density distribution of cloud base rain rate as a function of the ratio of *LWP* to cloud droplet number concentration (${LWP}/{N_d}$). The probability density distributions from all three regions have similar patterns, thus suggesting that drizzle formation processes of stratocumulus clouds in these subtropical subsidence flow regions are largely the same. Cloud base rain rates have a positive correlation with ${LWP}/{N_d}$ and rain rate increases become larger as ${LWP}/{N_d}$ becomes larger, which is consistent with our physical understanding that larger cloud droplet near the cloud top will enhance the raindrop embryo production through auto-conversion and subsequent accretion growth of raindrops. Larger ${LWP}/{N_d}$ implies larger cloud top droplet size because cloud top *LWC* has a positive correlation with *LWP* which is drawn from our assumption that *LWC* increases with geometrical height within the cloud layer with similar condensate rate. In the region of ${LWP}/{N_d}$ less than 1, the increase of R_{cb} with respect to ${LWP}/{N_d}$ becomes more gradual. This is also consistent with our physical understanding that cloud droplets need to be larger than certain size for auto-conversion to occur. Although the slope of rain rate with respect to ${LWP}/{N_d}$ is nearly the same as the results of Comstock et al. (2004) in the region of ${LWP}/{N_d}$ greater than 1, the absolute value of rain rate in this study is one order of magnitude smaller than that of Comstock et al. (2004). Since similar Z-R relations are employed to estimate cloud base rain rate from radar reflectivity in both studies, this is unlikely to have a large impact on the rain rate. It is more likely that the difference between these two studies comes from the overestimation of ${LWP}/{N_d}$. It is possible that *LWP* is overestimated or cloud droplet number concentrations are underestimated in this study, which result in the overestimation of ${LWP}/{N_d}$.

We now ask why such over- and underestimations are possible? Firstly, the physical meaning of the estimated cloud droplet concentration is different between these two studies. Comstock et al. (2004) employed cloud optical thickness and *LWP* obtained from ground-based pyranometer and microwave radiometer to compute cloud layer mean cloud droplet number concentrations. In this study, we estimate the near cloud top value from MODIS effective radius and cloud optical thickness. Although we assume vertically constant cloud droplet number concentration for the derivation, strictly speaking, it is not vertically constant in nature. Due to the collisions between cloud droplets, the expansion of air parcels and the evaporation caused by entrainment, cloud droplet number concentration tends to decrease as the altitude increases. Thus, satellite-derived cloud droplet concentrations are often smaller than those derived from ground-based observation.

Secondly, positive bias of MODIS cloud droplet radius leads to overestimation of *LWP* and underestimation of cloud droplet number concentration, both of which result in the overestimation of $^{LWP}/_{N_d}$ (See Eq. (2.13) and Eq. (2.14)). Comparing the MODIS effective radius and those observed by in-situ aircraft observation for northeast Pacific stratocumulus clouds, Stephen and Hudson (2015) found that MODIS effective radius of $2.1\mu m$ overestimates the cloud droplet size by 20-30% at cloud top. Since we are only analyzing those data satisfying $r_{e,3.7} > r_{e,2.1} > r_{e,1.6}$, the bias could be even more pronounced. Assuming that the overestimation of MODIS $r_{e,3.7}$ is 25% and the cloud droplet number concentration at cloud top is 65% of that of the cloud layer mean, $^{LWP}/_{N_d}$ derived in this study should be about 330% ($^{1.25}/_{(0.65 \times 1.25^{-2.5})} \approx 3.35$) larger than that of Comstock et al. (2004). Figure 3.2 shows the probability density distributions of cloud base rain rate and $^{LWP}/_{N_d}$ after correcting for the estimated differences in $^{LWP}/_{N_d}$. In the region where $^{LWP}/_{N_d}$ is greater than 1, the probability density distributions from the three regions now become much more similar to those of Comstock et al. (2004), which suggests that the ground-based study of Comstock et al (2004) and the satellite study conducted here are, in fact, consistent.

Figure 3.3 shows the cloud base rain rate as a function of ratio of *LWP* to cloud droplet number concentration ($^{LWP}/_{N_d}$) for various ranges of cloud droplet number concentration. All three

regions show similar patterns of high cloud droplet number concentration being located in the region of small $^{LWP}/_{N_d}$ ratios. Cloud base rain rate and the change in rain rate for these points with high cloud drop number concentrations are smaller compared to those with lower cloud droplet number concentrations, suggesting that the relation between cloud base rain rate and *LWP* can be differentiated by cloud droplet number concentration. It is important to sort the data by cloud droplet number concentration for discussing the dependency of cloud base rain rates on *LWP* and cloud droplet number concentration. Figure 3.4 shows that cloud base rain rate decreases with higher cloud droplet number concentration regardless of *LWP*, which demonstrates more clearly that higher cloud droplet number concentrations suppress the auto-conversion and accretion growth of rain droplets.

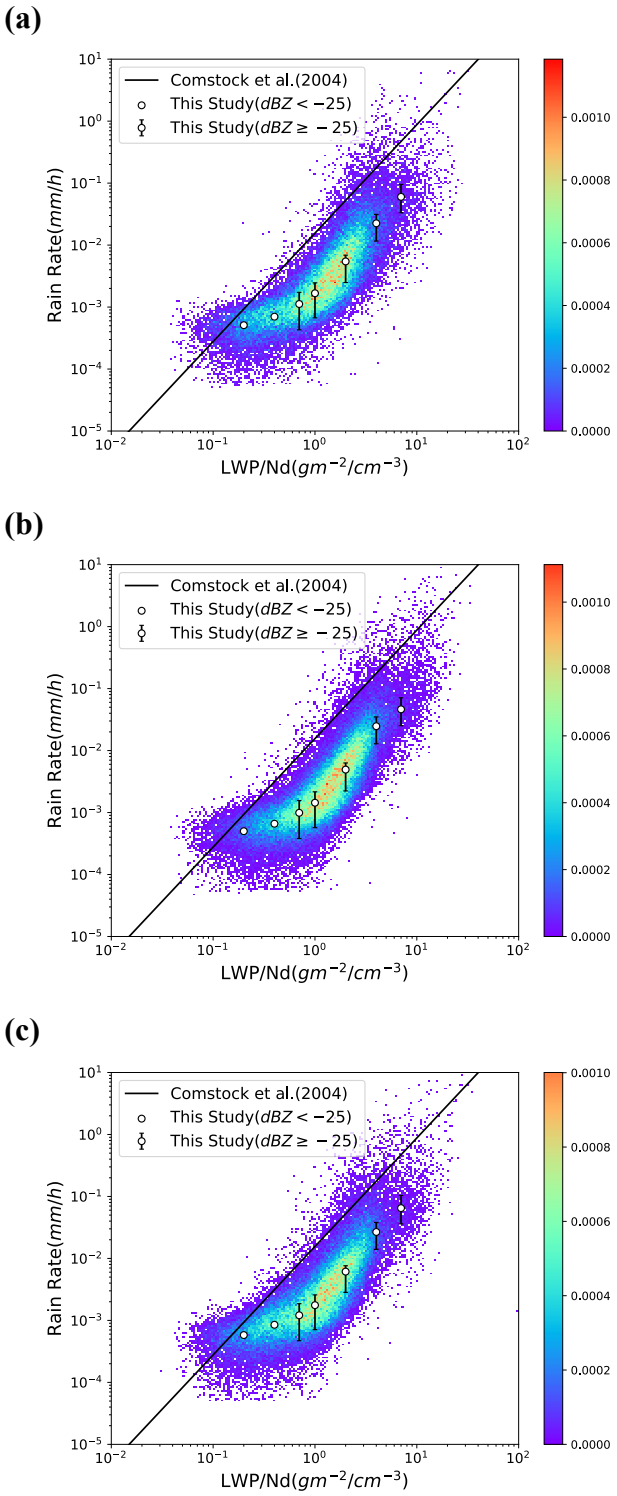

Figure 3.1 Probability density distributions of cloud base rain rate and the ratio of *LWP* to cloud droplet number concentration ($^{LWP}/_{N_d}$) for (a) NEP, (b) SEP and (c) SEA. White circles denote median cloud base rain rate. Relation presented in Comstock et al. (2004) is denoted in solid black lines.

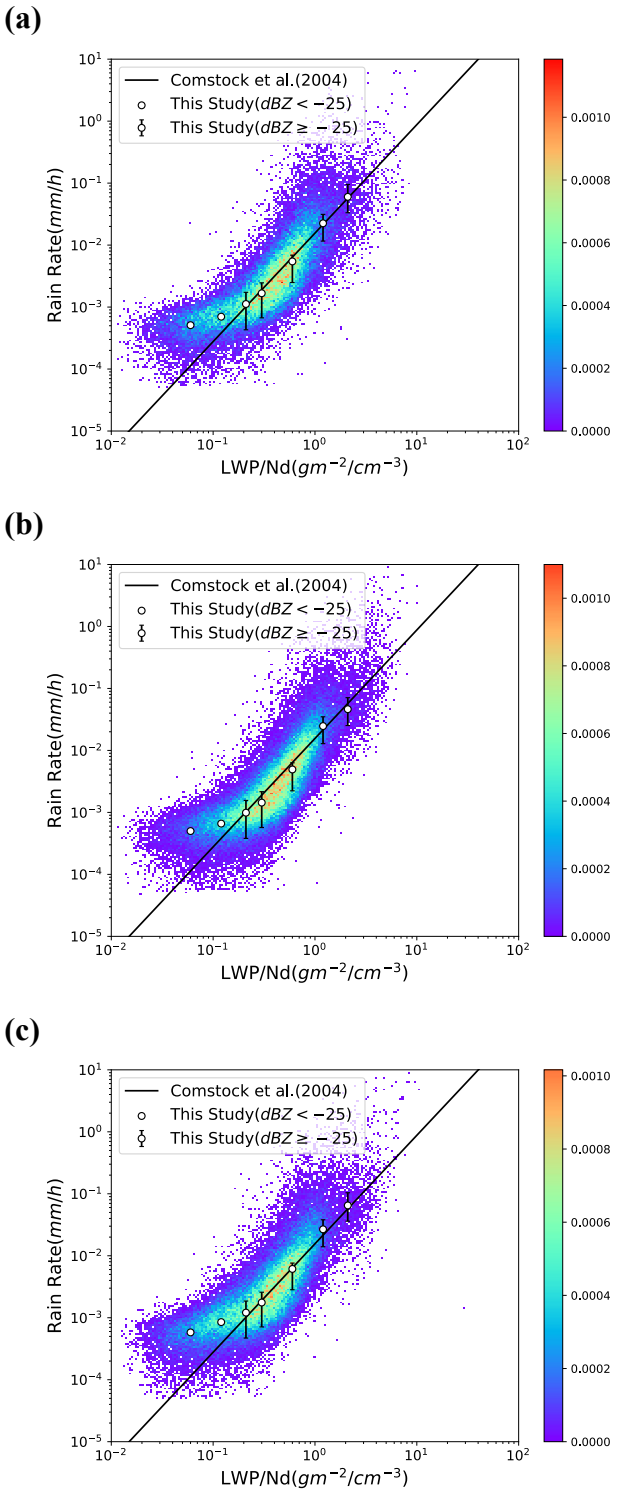

Figure 3.2 Same as Figure 3.1 but for when the data are corrected for biases arising from MODIS cloud droplet biases.

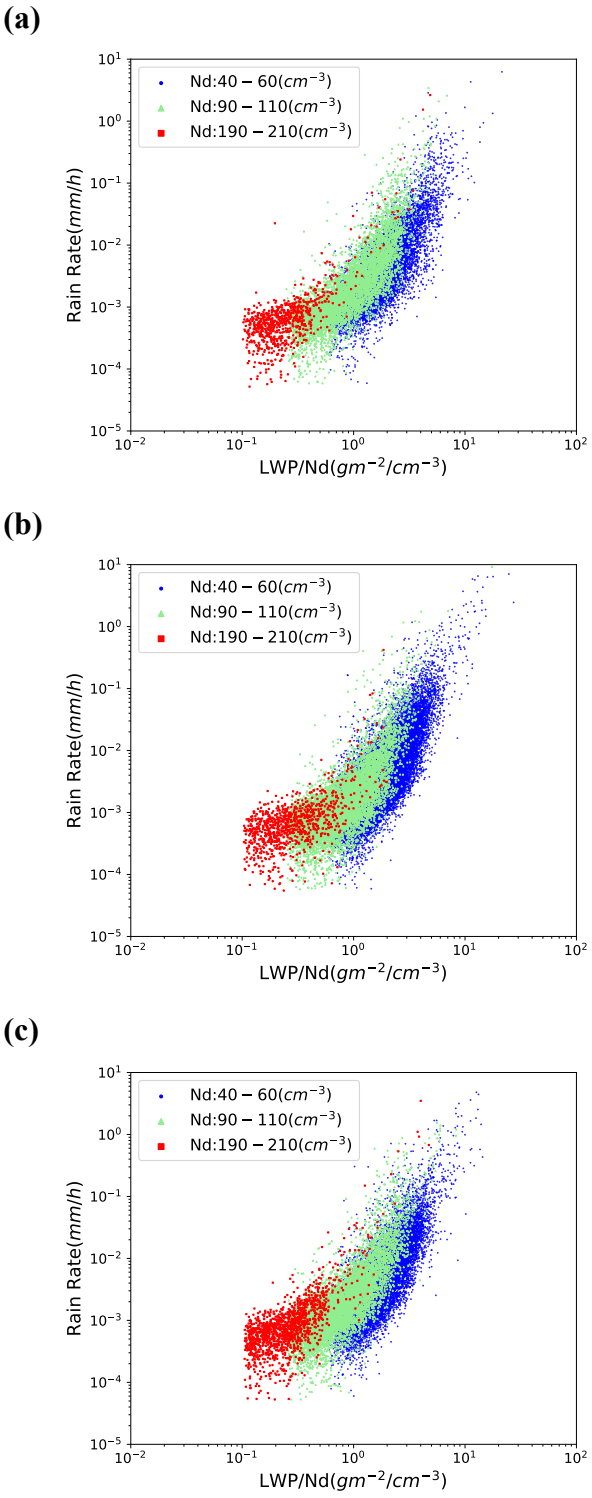

Figure 3.3 Cloud base rain rate as a function of the ratio of *LWP* to cloud droplet number concentration ($^{LWP}/_{N_d}$) for (a) NEP, (b) SEP and (c) SEA. Data are classified by cloud droplet number concentration; $40-60cm^{-3}$ (blue dot), $90-110cm^{-3}$ (green triangle) and $190-210cm^{-3}$ (red rectangle).

(a)

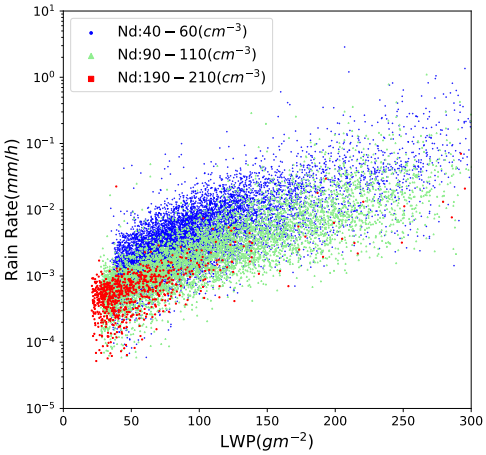

(b)

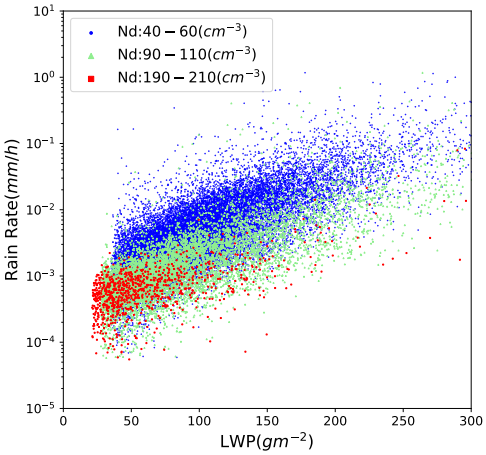

(c)

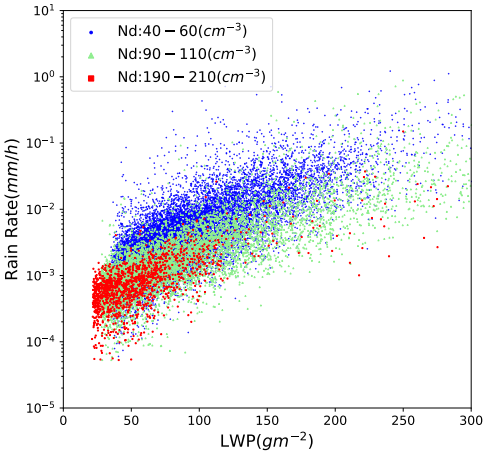

Figure 3.4 Cloud base rain rate as a function of LWP for (a) NEP, (b) SEP and (c) SEA. Notation of cloud droplet number concentration range are same as Figure 3.3.

Chapter 4

Dependency of auto-conversion rate on cloud droplet number concentration

4.1 Dependency of cloud base rain rate on cloud droplet number concentration

The absolute value of the auto-conversion rate as well as its response to cloud droplet number concentration is useful for improving the auto-conversion parameterization. In this chapter, the dependency of auto-conversion rates on cloud droplet number concentration is discussed based upon the dependency of cloud base rain rate on cloud droplet number concentration under constant LWC (LWP) assumptions.

Cloud base rain rate R_{cb} is generally written as Eq. (18):

$$R_{cb} = \frac{\pi}{6}\int N(r_{drizzle})\, r_{drizzle}^3 u(r_{drizzle}) dr_{drizzle} \tag{4.1}$$

where $N(r_{drizzle})$, $r_{drizzle}$ and $u(r_{drizzle})$ are the number concentration, radius and falling velocity of drizzle drops, respectively. As shown in Eq. (3.1), the auto-conversion rate is proportional to $N_d^{-\beta}$ under constant *LWC* conditions. From our assumption that auto-conversion produces raindrop embryos of similar size, it could be further approximated that number concentrations of raindrop embryos produced by auto-conversion should also be proportional to $N_d^{-\beta}$. Also, as shown in Eq. (3.2), under constant *LWP,* accretion growth of raindrops is proportional to the cloud-layer-mean collection efficiency. Finally, assuming that collection efficiency is independent of cloud droplet size and expressing the raindrop fall speed in the power-law form of $u(R) = aR^b$, the relation among cloud base rain rate, cloud droplet number concentration and cloud base raindrop size can be written as Eq. (4.2), where R is the mean cloud base raindrop radius ($r_{drizzle} = r_d$):

$$R_{cb} \propto N_{drizzle}\frac{4\pi}{3} r_d^3 a r_d^b \propto N_d^{-\beta} a r_d^{3+b} \tag{4.2}$$

Taking the logarithm of both sides of Eq. (4.2) gives Eq. (4.3).

$$\log R_{cb} \propto -\beta \log N_d + const. \tag{4.3}$$

It can be seen from Eq. (4.3) that the slope of the logarithm of the cloud base rain rate as a function of the logarithm of cloud droplet number concentration represents the dependency of auto-conversion rate on cloud droplet number concentration. Collision efficiency is fundamentally a function of cloud droplet number concentration. It becomes more (less) efficient with smaller (larger) cloud droplet number concentrations, which result in larger (smaller) raindrop at cloud base. Since data with smaller (larger) cloud droplet number concentrations will have stronger (weaker) rain rates at cloud base, the slope of log-log plot should be steeper than $-\beta$ of Eq. (4.3). Thus, the slope represents the upper-limit of dependency of auto-conversion on cloud droplet number concentration.

4.2 Results

In order to estimate the dependency of auto-conversion rate on cloud droplet number concentration from the current data, changes in the relation between cloud base rain rate and cloud droplet number concentration for different cloud top liquid water content and *LWP* are investigated. Figure 4.1 shows the cloud top (left panels) and cloud base (right panels) rain rate as a function of cloud droplet number concentration for different cloud top liquid water contents. The same Z-R relation is employed for the rain rate calculation at both cloud top and cloud base. Here, we assume that it is qualitatively valid to apply a Z-R relation, which is derived from cloud base and/or cloud-layer-mean droplet size distributions, to estimate cloud top rain rates since stratocumulus clouds are relatively thin and therefore droplet size distributions are relatively similar at both cloud top and cloud base. Cloud top liquid water content is calculated from Eq. (4.4) which assumes a linear increase in liquid water contents with height. It should be noted that the CloudSat radar observations contain some intrinsic uncertainty arising from its coarse vertical resolution of about 240 m and inability to observe cloud base height below 1km. There may be ways to accurately estimate the cloud top liquid water content by combining space-borne radar and lidar data, but it is left for future work.

$$LWC = \frac{2LWP}{H} \tag{4.4}$$

The relation between cloud base rain rate and cloud droplet number concentration for all three regions appears similar, suggesting that the response of the auto-conversion rate to cloud droplet number concentration in these subtropical subsidence regions are also similar. Regardless of cloud top liquid water contents, cloud top rain rate increases with decreasing cloud droplet number concentration at cloud top. This is consistent with our physical understanding as expressed in Eq. (3.1) that auto-conversion is enhanced by larger cloud droplets sizes. Clouds with cloud droplet number concentrations of more than $100\ cm^{-3}$ have similar small cloud base rain rates regardless of cloud top liquid water content, from which we infer that raindrop embryo formation through auto-conversion rarely occurs in these stratocumulus clouds. Cloud base rain rate is generally larger than that at cloud top but there is no significant difference between them for clouds with cloud droplet number concentration of more than $100\ cm^{-3}$. The growth of raindrops through the collection of cloud droplets occurs when significant numbers of raindrop embryos are produced by auto-conversion at cloud top, but these processes are not pronounced in clouds with high cloud droplet number concentrations, where cloud droplets are too small to produce raindrop embryos through auto-conversion. The difference between cloud top and cloud base rain rates increases with lower cloud droplet number concentrations and larger cloud top liquid water content, suggesting that collision-coalescence is more efficient in clouds with larger cloud droplets. Figure 4.2 shows the relation between cloud base rain rate and cloud droplet number concentration as a function of *LWP* for clouds with similar cloud top liquid water content ($LWC = 0.35 - 0.45\ g\ m^{-3}$). For clouds with similar cloud droplet number concentration, cloud base rain rate and its dependency on cloud droplet number concentration become stronger as *LWP* increases. This response of cloud base rain rate to *LWP* is consistent with Eq. (3.2) which suggests the accretion growth of raindrops is proportional to *LWP*. The increased dependency of cloud base rain rate on cloud droplet number concentration with increasing *LWP* reflects the cloud droplet size dependency on collection efficiency between raindrops and cloud droplets, which is larger for

clouds with larger cloud droplets (i.e. fewer cloud droplet number concentration). Based on these observations, it is inferred that clouds with small cloud top liquid water content or *LWP*, where raindrops experience less efficient accretion growth, are suitable for evaluating the dependency of auto-conversion rate on cloud droplet number concentration.

Figures 4.3 and 4.4 show the scatter plot and probability density distribution of cloud base rain rate and cloud droplet number concentration for stratocumulus clouds with cloud top liquid water content of $0.15 - 0.25\ g\ m^{-3}$ and *LWP* of $40 - 60\ g\ m^{-2}$. The range of cloud top liquid water content and *LWP* are chosen as robust samples while focusing on clouds with small liquid water contents. The black solid line indicates the linear regression line obtained from data with cloud droplet number concentration of $30 - 80\ cm^{-3}$. Since auto-conversion is suppressed in clouds with higher cloud droplet number concentrations, the inclusion of data with higher cloud droplet number concentrations could cause an underestimation of the dependency of the auto-conversion rate on cloud droplet number concentration. The estimated dependency of cloud base rain rate on cloud droplet number concentration is an exponent of -1.328, -1.552 and -1.440 for SEA, SEP and SEA respectively. To the best of the author's knowledge, the range of $-\beta$ in Eq. (3.1), which corresponds to the estimated dependency, is largely varying from $-1/3$ (Kesler, 1969) to -1.79 (Khairoutdinov and Kogan, 2000, hereafter KK) depending on the parametrization schemes. The result of this study is closer to that of KK which is based on LES result assuming cloud droplet size distribution for stratocumulus clouds. Wood (2005) performed a stochastic collision-coalescence calculation assuming cloud droplet size distribution obtained by in-situ aircraft measurements of stratocumulus clouds and found that KK's scheme properly reproduces the auto-conversion rate in stratocumulus clouds. The result of this study, obtained from a different approach, also supports the finding of the Wood's study. Although the dependency of the auto-conversion rate on cloud droplet number concentration shows some regional variability of about ± 0.1, it seems that β is smaller than KK's value of 1.79 within the range of *LWP* and cloud droplet number concentration used in this analysis.

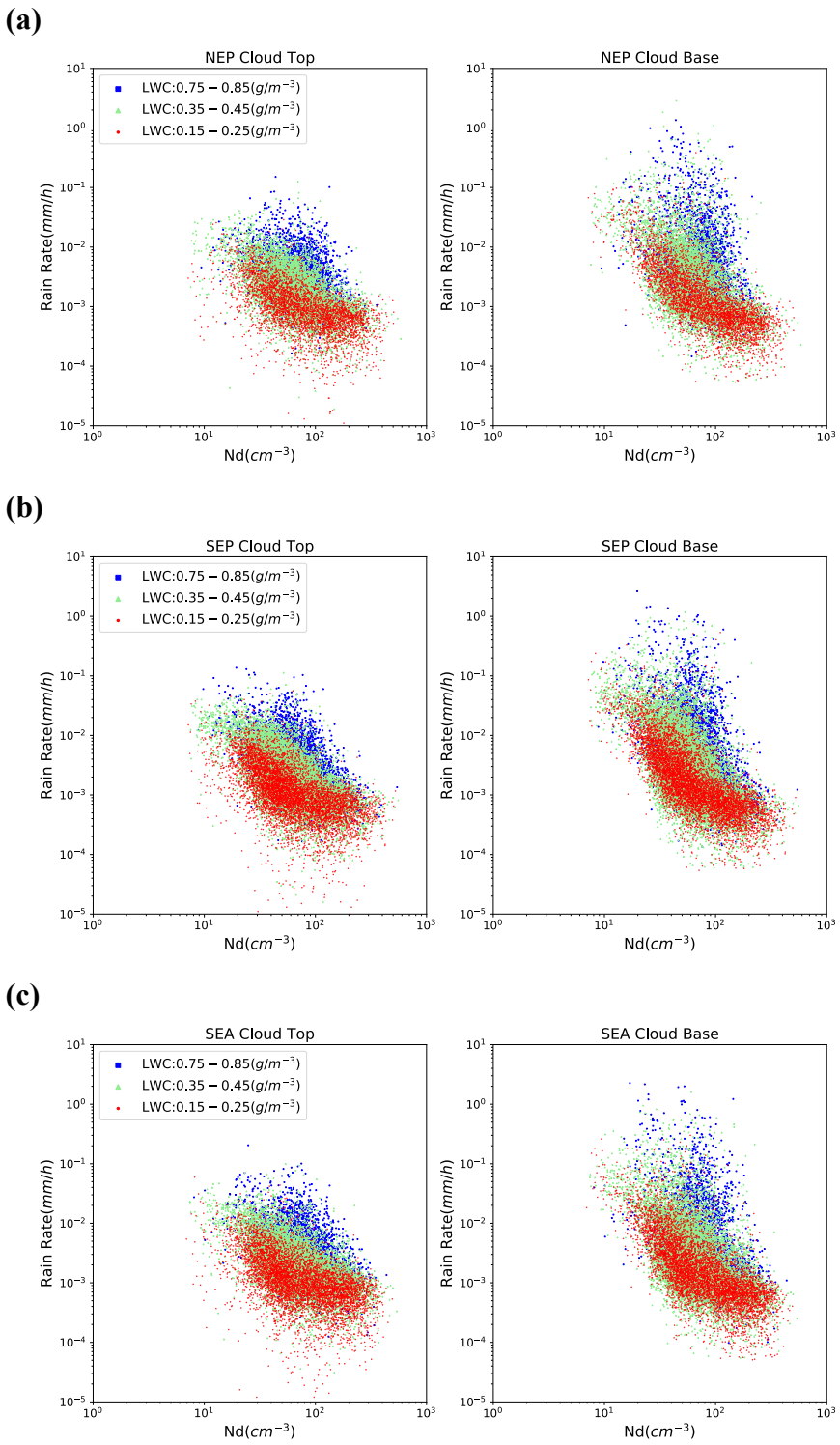

Figure 4.1 Cloud top (left panels) and cloud base (right panels) rain rate as a function of cloud droplet number concentration for different cloud top liquid water contents for (a) NEP, (b) SEP and (c) SEA.

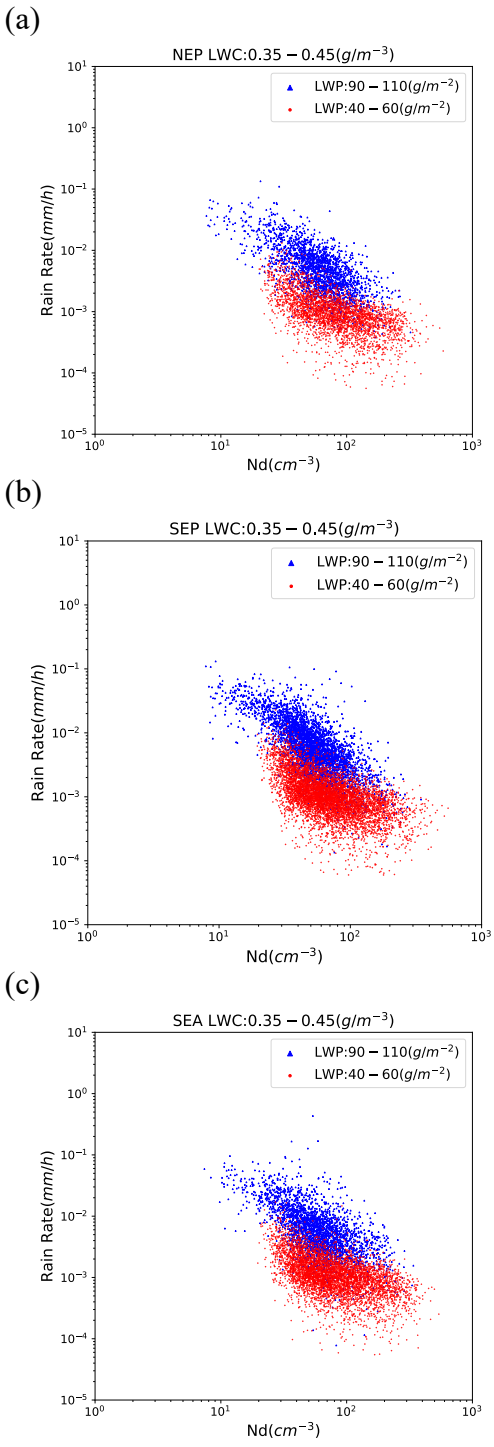

Figure 4.2 Relations between cloud base rain rate and cloud droplet number concentration as a function of *LWP* for clouds with similar cloud top liquid water content (LWC = $0.35 - 0.45\ g\ m^{-3}$) for (a) NEP, (b) SEP and (c) SEA.

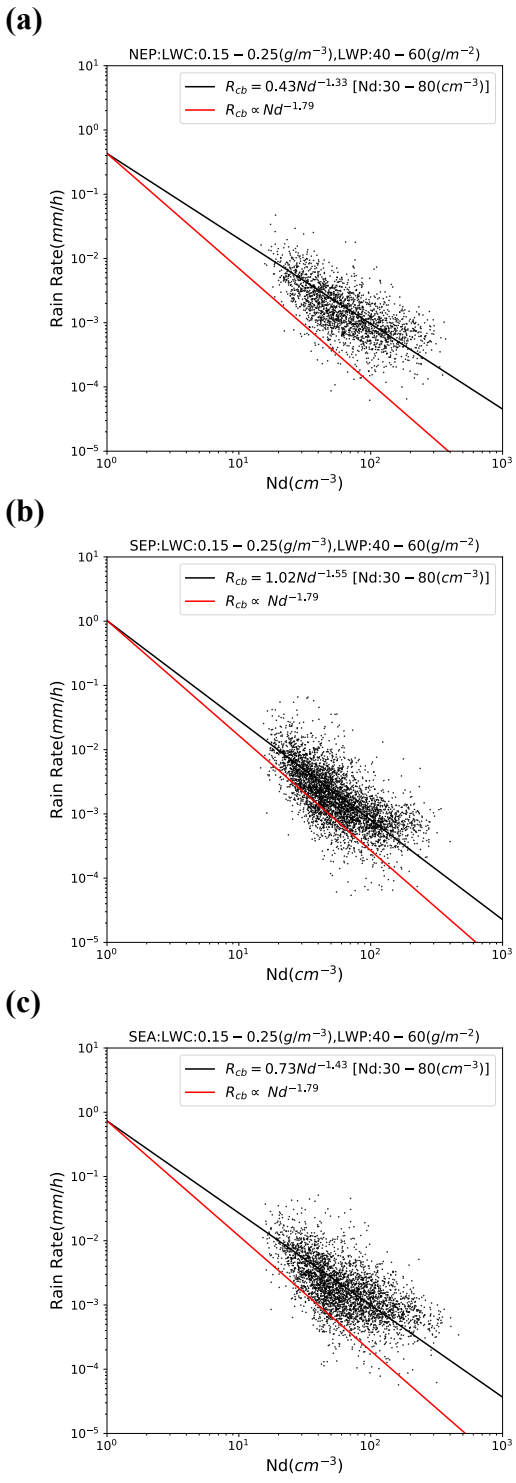

Figure 4.3 Scatter plots of cloud base rain rate and cloud droplet number concentration for (a) NEP, (b) SEP and (b) SEA. Black solid line indicates the linear regression line obtained from data with cloud droplet number concentration of $30 - 80\ cm^{-3}$. Red solid line denotes the dependency of auto-conversion rate on cloud droplet number concentration in Kogan (2000).

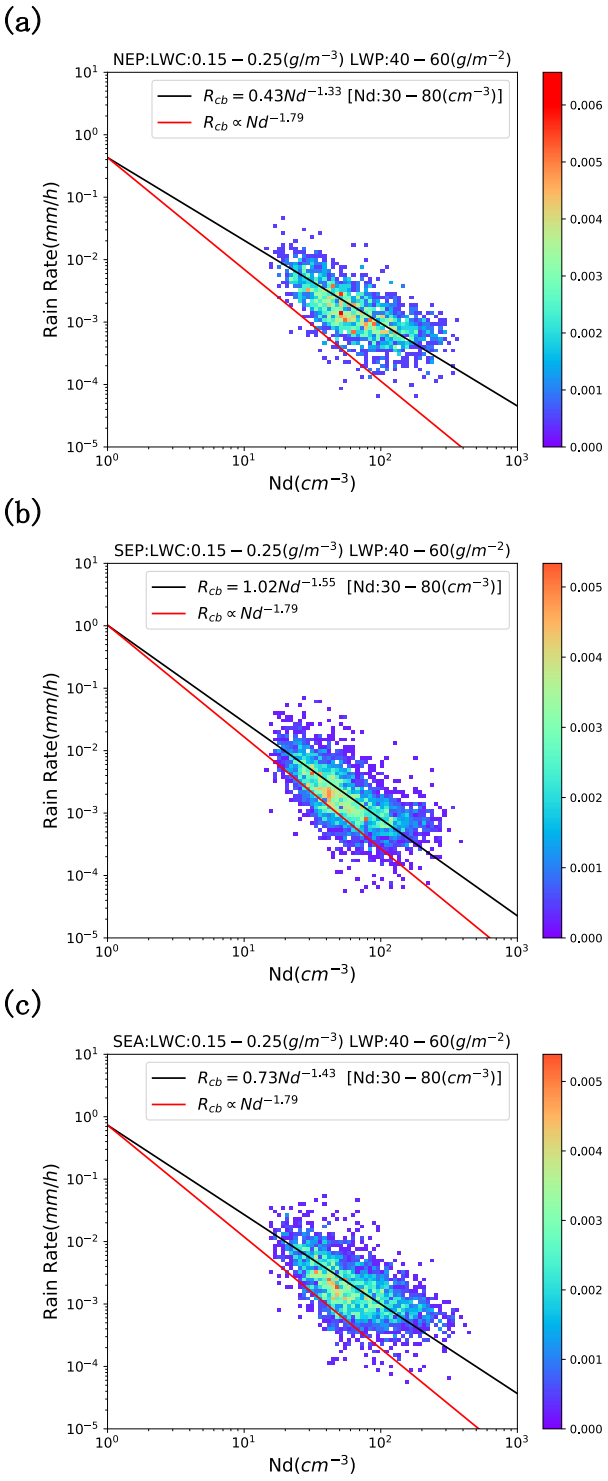

Figure 4.4 Same as Figure 4.3 but for probability density distribution.

Chapter 5

Summary and future work

In this study, large amounts of space-borne observations from A-Train satellites are utilized to obtain relations among liquid water path, cloud droplet number concentration and the cloud base rain rate for three regions with similar environments, namely the northeast Pacific off the coast of California, the southeast Pacific off the coast of Peru and the southeast Atlantic off the coast of Namibia. These regions are selected as they represent areas where strong subsidence associated with the subtropical-high is prevalent.

Radar reflectivity from the CloudSat Cloud Profiling Radar (CPR) is employed to estimate cloud base rain rate. Liquid water path (*LWP*) and cloud droplet number concentration (*Nd*) are estimated from MODIS cloud optical thickness and effective radius. We obtain the relation between cloud base rain rate (R_{cb}) and the ratio of *LWP* to cloud droplet number concentration ($^{LWP}/_{N_d}$) and investigate its response to cloud droplet number concentrations. The relations for all three regions show similar patterns. Satellite observations show that R_{cb} is positively correlated with $^{LWP}/_{N_d}$, which agrees with previous studies. It is also found that the R_{cb} has an increasing trend with larger ratios of $^{LWP}/_{N_d}$.

This study also demonstrated that the cloud base rain rate and its rate of change with respect to the ratio of *LWP* to cloud droplet number concentration ($^{LWP}/_{N_d}$) is larger for clouds with lower cloud droplet number concentrations, and pointed out the possibility that the relation between cloud base rain rate and *LWP* can be stratified by the cloud droplet number concentration. These findings are consistent with our theoretical understanding of 1) auto-conversion and the accretion growth of raindrop embryos that become more effective as droplet number concentrations near cloud top cloud become smaller, and 2) auto-conversion is suppressed when the cloud droplet radius is small enough.

When compared to the results of Comstock et al. (2004), it was found that the changes of the cloud base rain rate with respect to $^{LWP}/_{N_d}$ are nearly the same in the region of $^{LWP}/_{N_d}$ greater

than 1, whereas the absolute value of cloud base rain rate in this study is one order of magnitude smaller than that the Comstock et al. (2004) study. We have shown that this difference can be explained by two reasons. Firstly, a positive bias of the MODIS cloud droplet radius leads to an overestimation of the *LWP* and an underestimation of cloud droplet number concentration. Secondly, the physical meaning of the cloud droplet number concentration is different in these two studies. The results of this study represent number concentrations at cloud top whereas the Comstock et al. (2004) in-situ values represent cloud-layer-averaged values.

The upper limit of the dependency of auto-conversion on cloud droplet number concentration (i.e. β in Eq. (3.1)) is discussed by investigating the response of cloud base and cloud top rain rates to cloud droplet number concentrations for stratocumulus clouds with smaller cloud top *LWCs* (*LWPs*). These clouds are chosen because their raindrops are less sensitive to the collection growth of cloud droplets. β is found to be -1.44 ± 0.12 in this study. This result suggests that the dependency of the auto-conversion rate in stratocumulus clouds on cloud droplet number concentration is greatly underestimated in Kessler type parametrizations which assume $\beta = {}^{1}/_{3}$, whereas the parametrization presented by Khairoutdinov and Kogan (2000) which assumes $\beta = 1.79$ is somewhat overestimating it.

In this study, we have focused only on stratocumulus clouds that develop in subtropical subsidence regions, but there are many other environments where stratocumulus clouds exist such as baroclinic storm systems and cold-air outbreaks in the mid-latitudes. It is therefore important to also analyze the stratocumulus clouds formed in those environments to further understand the behavior of auto-conversion. Since entrainment rate and cloud vertical structures are expected to vary with environments, estimates of cloud droplet number concentration and liquid water content at cloud top may differ from the assumptions used in this study. It will therefore be important to estimate these variables without assuming dependency on the vertical structure of clouds, which could be achieved by combining space-borne radar and lidar observations. This study also showed that the precipitation processes of stratocumulus clouds differ by liquid water content and cloud droplet number concentration at cloud top. Inter-comparisons of satellite-derived and model-

simulated auto-conversion rates by dividing these parameters into different value ranges will be also interesting.

References

Ackerman, A. S., O. B. Toon, D. E. Stevens, and J. A. Coakley Jr., 2003: Enhancement of cloud cover and suppression of nocturnal drizzle in stratocumulus polluted by haze. *Geophys. Res. Lett.*, **30**, 1381, doi: 10.1029/2002GL016634.

Abel, S. J., D. N. Walters, and G. Allen, 2010: Evaluation of stra-tocumulus cloud prediction in the Met Office forecast model during VOCALS-REx. *Atmos. Chem. Phys.*, **10**, 10541–10559, doi: 10.5194/acp-10-10541-2010.

Albrecht, B. A., 1989: Aerosols, cloud microphysics, and fractional cloudiness. *Science*, **245**, 1227–1230.

Albrecht, B. A., R. P. Penc, and W. H. Schubert, 1985: An observational study of cloud-topped mixed layer. *J. Atmos. Sci.*, **42**, 800– 822, doi: 10.1175/1520-0469(1985)042<0800:AOSOCT>2.0.CO;2.

Bennartz, R. and J. Rausch, 2017: Global and regional estimates of warm cloud droplet number concentration based on 13 years of AQUA-MODIS observations, *Atmos. Chem. Phys.*, **17**, 9815–9836, doi: 10.5194/acp-17-9815-2017.

Boers, R., J. B. Jensen, and P. B. Krummel, 1998: Microphysical and short-wave radiative structure of stratocumulus clouds over the Southern Ocean: Summer results and seasonal differences. *Quart. J. Roy. Meteor. Soc.*, **124**, 151– 168.

Brenguier, J. L., H. Pawlowska, L. Schuller, R. Preusker, J. Fischer, and Y. Fouquart, 2000: Radiative properties of boundary layer clouds: Droplet effective radius versus number concentration. *J. Atmos. Sci.*, **57**, 803–821.

Comstock, K. K., R. Wood, S. E. Yuter, and C. S. Bretherton, 2004: The relationship between reflectivity and rain rate in and below drizzling stratocumulus. *Quart. J. Roy. Meteor. Soc.*, **130,** 2891–2918.

Geoffroy, O., J. L. Brenguier, and I. Sandu, 2008: Relationship between drizzle rate, liquid water path and droplet concentration at the scale of a stratocumulus cloud system. *Atmos. Chem. Phys*., **8**, 4641–4654.

Grosvenor, D. P., and Coauthors, 2018: Remote sensing of droplet number concentration in warm clouds: A review of the current state of knowledge and perspectives. *Rev. Geophys.*, **56**, 409–453

Hansen, J., and L. Travis, 1974: Light scattering in planetary atmospheres. *Space Science Reviews*, **16(4)**, 527– 610, doi: 10.1007/BF00168069.

Ishizaka, Y., Y. Kurahashi, and H. Tsuruta, 1995: Microphysical properties of winter stratiform clouds over the southwest island area in Japan. *Journal of the Meteorological Society of Japan*, **73**, 1137– 1151, doi: 10.2151/jmsj1965.73.6_1137.

Jiang, H., G. Feingold, and W. R. Cotton, 2002: Simulations of aerosol-cloud-dynamical feedbacks resulting from entrainment of aerosol into the marine boundary layer during the Atlantic

Stratocumulus Transition Experiment. *J. Geophys. Res.*, **107,** 4813, doi: 10.1029/2001JD001502.

Khairoutdinov, M., and Y. Kogan, 2000: A new cloud physics parameterization in a large-eddy simulation model of marine stratocumulus. *Monthly Weather Review*, **128**, 229– 243.

Klein, S. A., and D. L. Hartmann, 1993: The seasonal cycle of low stratiform clouds. *J. Climate*, **6**, 1587–1606.

Klein, S. A., and Coauthors, 2009: Intercomparison of model simulations of mixed-phase clouds observed during the ARM Mixed-Phase Arctic Cloud Experiment. I: Single-layer cloud. *Quart. J. Roy. Meteor. Soc.*,**135**, 979–1002.

Leon, D. C., Z. Wang, and D. Liu, 2008: Climatology of drizzle in marine boundary layer clouds based on 1 year of data from CloudSat and Cloud-Aerosol Lidar and Infrared Pathfinder Satellite Observations (CALIPSO). *J. Geophys. Res.*, **113**, D00A14, doi: 10.1029/2008JD009835.

Liebe, H. J., T. Manabe and G.A. Hufford, 1989: Millimeter-wave attenuation and delay rates due to fog/cloud conditions. I*EEE Trans. Antenn. Prop.*, **37**, 1617-1623.

Liu, Y., and P. H. Daum, 2004: On the parameterization of the au-toconversion process. Part I: Analytical formulation of the Kessler-type parameterizations. *J. Atmos. Sci.*, **61**, 1539–1548.

Mace, G. G., and Q. Zhang, 2014: The CloudSat radar-lidar geometrical profile product (RL-GeoProf): Updates, improvements, and selected results. *J. Geophys. Res. Atmos.*, **119**, doi: 10.1002/ 2013JD021374.

Marchand, R., G.G. Mace, T. Ackerman, and G. Stephens, 2008: Hydrometeor Detection Using Cloudsat—An Earth-Orbiting 94-GHz Cloud Radar. *J. Atmos. Oceanic Technol.*, **25**, 519–533.

Martin, G. M., D. W. Johnson, and A. Spice, 1994: The measurement and parameterization of effective radius of droplets in warm stratocumulus clouds. *J. Atmos. Sci.*, **51**, 1823–1842, doi: 10.1175/1520-0469(1994)051<1823:TMAPOE>2.0.CO;2

Min, Q., E. Joseph, Y. Lin, L. Min, B. Yin, P. H. Daum, et al., 2012: Comparison of MODIS cloud microphysical properties with in-situ measurements over the Southeast Pacific. *Atmos. Chem. Phys.*, **12**, 11261–11273, doi: 10.5194/acp-12-11261-2012.

Muhlbauer, A., I. L. McCoy, and R. Wood, 2014: Climatology of stratocumulus cloud morphologies: microphysical properties and radiative effects, *Atmos. Chem. Phys.*, **14**, 6695–6716, doi: 10.5194/acp-14-6695-2014.

Nicholls, S. and J. Leighton, 1986: An observational study of the structure of stratiform cloud sheets: Part I. Structure. *Quart. J. Roy. Meteor. Soc.*, **112**, 431–460.

Noble, S. R., and J. G. Hudson, 2015: MODIS comparisons with northeastern Pacific in situ stratocumulus microphysics. *J. Geophys. Res.: Atmos.*, **120**, 8332– 8344, doi: 10.1002/2014JD022785.

Painemal, D., and P. Zuidema, 2011: Assessment of MODIS cloud effective radius and optical thickness retrievals over the Southeast Pacific with VOCALS-REx in situ measurements. *J. Geophys. Res.* **116**, D24206, doi: 10.1029/2011JD016155.

Platnick, S., and Coauthors, 2017: The MODIS Cloud Optical and Microphysical Products: Collection 6 Updates and Examples From Terra and Aqua. *IEEE Trans. Geosci. Remote Sens.*, **55(1)**, 502-525.

Rogers, D. P., and J. W. Telford, 1986: Metastable stratus tops. *Quart. J. Roy. Meteor. Soc.*, **112**, 481– 500, doi: 10.1002/qj.49711247211.

Rossow, W.B., and R.A. Schiffer, 1991: ISCCP Cloud Data Products. *Bull. Amer. Meteor. Soc.*, **71**, 2-20.

Slingo, A., 1990: Sensitivity of the Earth's radiation budget to changes in low clouds. *Nature*, **343,** 49–51.

Twomey, S., 1959: The supersaturation in natural clouds and the variation of cloud droplet concentration. *Geofis. Pura Appl.,* **43,** 243–249.

Vali, G., and S. Haimov, 2001: Observed extinction by clouds at 95 GHz. *IEEE Trans. Geosci. Remote Sens.*, **39(1)**, 190-193.

vanZanten, M. C., B. Stevens, G. Vali, and D. Lenschow, 2005: Observations ofdrizzle in nocturnal marine stratocumulus. *J. Atmos. Sci.*, **62**, 88–106.

Wang, H., P. J. Rasch, and G. Feingold, 2011: Manipulating marine stratocumulus cloud amount and albedo: a process-modelling study of aerosol-cloud-precipitation interactions in response to injection of cloud condensation nuclei, *Atmos. Chem. Phys.*, **11**, 4237–4249, doi: 10.5194/acp-11-4237-2011.

Wood, R., 2005a: Drizzle in stratiform boundary layer clouds. PartI: Vertical and horizontal structure. *J. Atmos. Sci.*, **62**, 3011–3033.

Wood, R., 2005b: Drizzle in stratiform boundary layer clouds. PartII: Microphysics aspects. *J. Atmos. Sci.*, **62**, 3034–3050, doi: 10.1175/JAS3530.1.

Wood, R, 2012: Stratocumulus clouds. *Mon. Wea. Rev.*, **140**, 2373–2423.